Available online at www.sciencedirect.com
SCIENCE DIRECT®
ELSEVIER
Journal of Magnetism and Magnetic Materials 301 (2006) 495–502
Journal of magnetism and magnetic materials
www.elsevier.com/locate/jmmm

Characterization of magnetic phases in the $Fe_xMn_{0.65-x}Al_{0.35}$ disordered alloys

Ligia E. Zamora[a], G.A. Pérez Alcázar[a,*], C. González[a], J.M. Greneche[b], W.R. Aguirre[a], A. Bohórquez[a], E.M. Baggio Saitovich[c], D. Sánchez[c]

[a]*Departamento de Física, Universidad del Valle, A. A. 25360, Cali, Colombia*
[b]*Laboratoire de Physique de L'Etat Condensé, UMR CNRS 6087, Université du Maine, 72085 Le Mans, Cedex 9, France*
[c]*Centro Brasileiro de Pesquisas Físicas, CBPF, Río de Janeiro, Brasil*

Received 4 April 2005
Available online 26 August 2005

Abstract

Melted alloys of the $Fe_xMn_{0.65-x}Al_{0.35}$ disordered system, $0.25 \leqslant x \leqslant 0.65$, were experimentally studied by Mössbauer spectrometry, vibrating sample magnetometry and AC magnetic susceptibility. All the alloys exhibit the BCC structure with a nearly constant lattice parameter (2.92 Å). Mössbauer studies at room temperature (RT) show that in the $0.25 \leqslant x \leqslant 0.45$ range the alloys are paramagnetic (P) while in the $0.50 \leqslant x \leqslant 0.65$ range, they are ferromagnetic. At 77 K, Mössbauer studies show that the alloy with $x = 0.25$ presents weak magnetic character that is consistent with an antiferromagnetic (AF) behavior due to the high Mn content, while those with $0.30 \leqslant x \leqslant 0.40$ are paramagnetic, and those in the $0.45 \leqslant x \leqslant 0.65$ range are ferromagnetic (F) with a mean field increasing with the Fe content. Hysteresis cycles at RT prove the paramagnetic character of the alloys between $x = 0.25$ and 0.40 and the ferromagnetic character for $x \geqslant 0.45$. Complementary measurements using AC magnetic susceptibility permit a magnetic phase diagram to be proposed, with the P phase for high temperature and all the compositions, the AF phase for low Fe content and at low temperature, the F phase for high Fe content above RT and the spin glass phase for all the compositions and at temperatures lower than 46 K. In addition, the mean field renormalization group (MFRG) method, applied to a random competitive and site dilute Ising model with nearest-neighbor, gives rise to magnetic phase diagram, which fairly agrees with previous experimental one.

PACS: 76.80; 75.30; 61.10

Keywords: Alloys; Hyperfine interactions; Magnetization; Mechanical alloying

*Corresponding author. Tel.: +57 2 3307627; fax: +57 2 3393237.
E-mail address: geperez@univalle.edu.co (G.A. Pérez Alcázar).

0304-8853/$ - see front matter © 2005 Elsevier B.V. All rights reserved.
doi:10.1016/j.jmmm.2005.08.005

1. Introduction

The Fe–Mn–Al system has been hardly studied due to the possibility to be used as stainless steel [1–3]. When Chakrabarti's method [4] is used to prepare them, disordered alloys are obtained and they present a large scientific interest due to the different types of magnetic phases that can be detected. Ferromagnetic (F) and paramagnetic (P) phases were earlier reported [5,6]. The occurrence of the spin-glass (SG) and reentrant-spin glass in the F and antiferromagnetic (AF) phases (RSG-F and RSG-AF, respectively) behaviors were theoretically proposed by Rosales Rivera et al. [7]. The SG and RSG-F phases were experimentally proved by Kobeissi [8], Zamora et al. [9,10] and Bremers [11]. These two phases result from both the disorder and the presence of competing F and AF interactions. Recently, an experimental magnetic phase diagram was also proposed for the $Fe_xMn_{0.3}Al_{0.7-x}$ ($0.275 \leqslant x \leqslant 0.525$) alloys system [12]. This phase diagram includes the P, F, and RSG-F phases and also AF and RSG-AF phases for high Mn contents. The occurrence of superparamagnetic-like (SP) blocked events was reported for temperatures above the AF phase. More recently, a magnetic phase diagram was established for the $Fe_xMn_{0.6-x}Al_{0.4}$ alloys system [13]: all the previous phases were observed, but a new phase was found in the Fe-rich region. It was attributed to reentrant SP behavior (RSP).

From the theoretical point of view, it is well established that Ising-like models are well suited to describe the critical behavior of many magnetic systems [14–16]. The renormalization groups [17] and the mean field renormalization group (MFRG) [18–20] techniques have been used in the study of the critical properties of magnetic systems. The MFRG method has been applied to pure, diluted, random-bond and random-field systems [20], as well as to a diluted and random-bond model [21]. These calculations have been successfully achieved to interpret the different experimental magnetic properties obtained for Fe–Al [22] and Fe–Mn–Al alloys in the BCC disordered phase [23], even regarding the SG and RSG zones of the phase diagrams.

Consequently, the aim of the present work is to report an experimental study of the magnetic and structural properties of powders of melted alloys of the $Fe_xMn_{0.65-x}Al_{0.35}$ system, with $0.25 \leqslant x \leqslant 0.60$, based on ^{57}Fe Mössbauer spectrometry (MS), X-ray diffraction (XRD), vibrating sample magnetometer (VSM) and AC susceptibility measurements. In addition, a theoretical study using a random site and diluted Ising model and the MFRG technique is proposed to describe the magnetic phase diagram for this system.

2. Experimental procedure

The samples were prepared by melting high purity Fe, Al and Mn powders in an arc furnace and under argon atmosphere. The melted materials were heated at 1000 °C for 1 week in evacuated quartz tubes and subsequently quenched in ice water. Powder prepared by crushing the quenched buttons was used for all the experimental measurements. Transmission Mössbauer spectra (MS) were recorded at 300 K and at 77 K using a constant acceleration spectrometer with a ^{57}Co/Rh source and a bath cryostat. The spectra were fitted using the MOSFIT program [25] including a discrete hyperfine field distribution (HFD) and, in most of the cases, additional paramagnetic components. The values of isomer shift are referred to that of natural Fe. The AC susceptibility measurements were carried out in a SQUID magnetometer, under an AC field of amplitude 3×10^{-4} T, a biasing DC field of 0.001 T and at a frequency of 20 Hz. For $x = 35$ the dependence of the susceptibility with the frequency (20–1500 Hz) was also studied. The hysteresis cycles were obtained using a conventional VSM with a maximum field of 0.65 T.

3. Experimental results and discussion

X-ray measurements proved that all the alloys unambiguously exhibit a BCC structure. The lattice parameter is nearly constant with a value of ≈ 2.92 Å, larger than that of the pure Fe due to the bigger size of Al atoms.

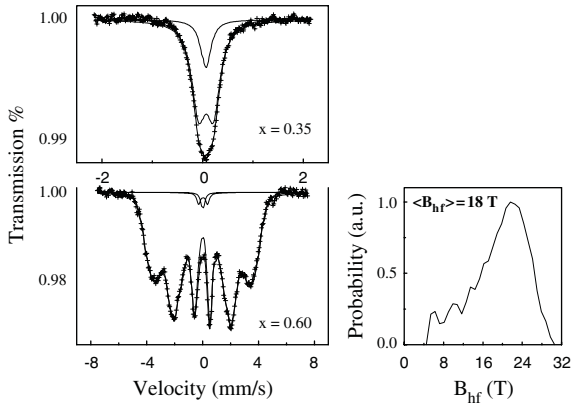

Fig. 1. Mössbauer spectra for the $x = 0.35$ and $x = 0.60$ samples at room temperature.

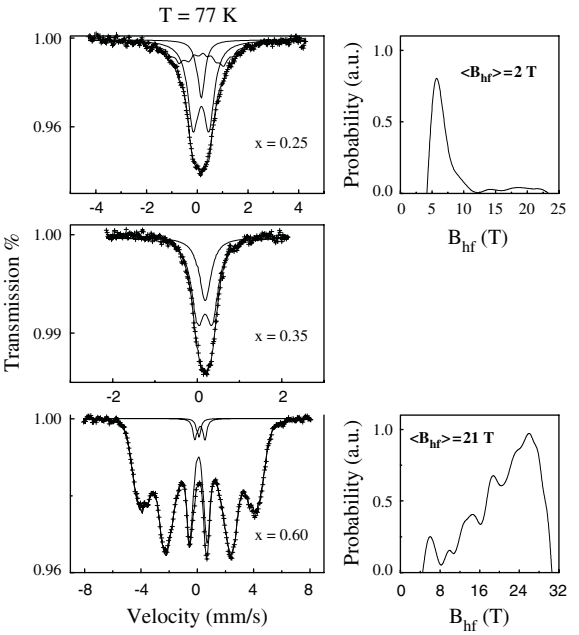

Fig. 2. Mössbauer spectra for the $x = 0.25$, 0.35 and $x = 0.60$ samples at 77 K.

Fig. 1 shows some MS recorded at 300 K for $x = 0.35$ (typical spectrum for samples in the range $0.25 \leqslant x \leqslant 0.45$) and for $x = 0.60$ (typical spectrum for samples in the $0.50 \leqslant x \leqslant 0.60$ range). The spectra of the first range were fitted by using a single line and a quadrupolar doublet, showing that these alloys are paramagnetic with two Fe components. MS spectra for alloys in the second range were fitted with a HFD, a quadrupolar doublet and a single line and that of $x = 0.65$ only with a HFD, showing that in this composition range the alloys are disordered and ferromagnetic. However, for $x = 0.65$ all the sites are ferromagnetic while for $x < 0.65$ additional P lines are detected. These P lines correspond to Fe-rich sites in Al and Mn atoms as nearest neighbors. For $x \geqslant 0.50$ the calculated mean HF obtained from the fit as a function of the Fe content increases with the increase in the Fe content. The mean isomer shift (δ) for the single line slightly decreases when the Fe concentration increases, with values of 0.22 ± 0.02 mm/s for $x = 0.25$ until 0.15 ± 0.022 mm/s for $x = 0.60$ i.e. the substitution of Mn atoms by Fe atoms increases δ. Indeed, the s electron density increases as the number of Fe atoms increases. Similar behaviors are observed for the other phases.

Three typical MS recorded at 77 K on samples with $x = 0.25$, 0.35 and 0.60 are shown in Fig. 2. The spectra for alloys with $x = 0.25$ and 0.30 were fitted with an additional low mean field HFD, which is associated with an AF order, in agreement with the high Mn content and with previous experimental reports [13] using AC magnetic susceptibility and calorimetry in alloys near this composition range. The spectra of the samples $x = 0.35$ and 0.40 were fitted with a quadrupolar doublet and a single line showing that their P character remains at 77 K. The spectra in the range $0.45 \leqslant x \leqslant 0.60$ were fitted with a HFD with high mean HF, a quadrupolar doublet and a single line and that with $x = 0.65$ with only a HFD with large mean HF value. MS of the $x = 0.25$ sample without and with a 0.04 T external field were performed at 77 K, as previously reported in Ref. [24]. These spectra and their HFDs are very similar and do not suggest the presence of any significant dynamical effects. These results suggest the AF character of the sample. MS and their corresponding HFDs, at 300 K, of the $x = 0.60$ sample without and with a 0.3 T external field (applied perpendicularly to the direction of γ-beam) were also previously performed [24]. The increase of the intermediate lines intensities ($\Delta m = 0$) is consistent with a ferromagnetic behavior while a shift to higher fields of the HFD (≈ 3 T) is larger than the external field suggests the presence of SP

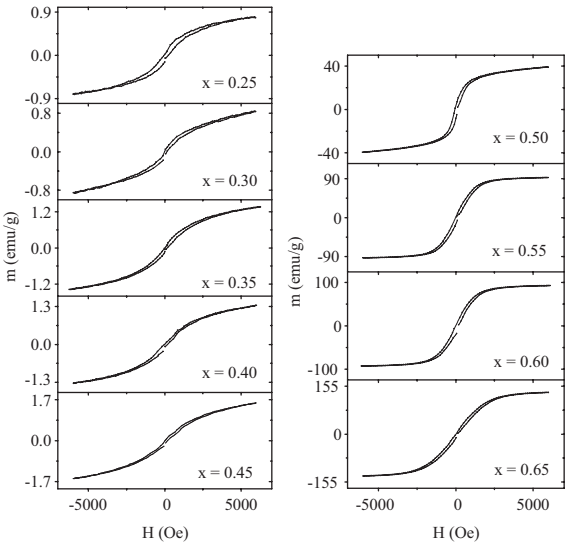

Fig. 3. Hysteresis curves for $Fe_xMn_{0.65-x}Al_{0.35}$ samples at room temperature.

relaxation effects. These results thus allow one to conclude that the $x = 0.60$ sample is F and presents dynamics attributed to SP cluster effects, probably to a RSP, as was detected for Fe-rich samples with 40 at% Al [13].

Fig. 3 shows the hysteresis cycles obtained at 300 K for all the samples using a maximum field of 0.65 T. It can be noted that samples with $x \leqslant 0.45$ present low-magnetization values (≈ 1 emu/g) and do not present saturation magnetization at 0.6 T, while those with $x \geqslant 0.50$ present high-magnetization values and saturation magnetization, 39 emu/g for $x = 0.50$ increasing with the Fe content up to 132 emu/gm for $x = 0.65$. These results, in agreement with the Mössbauer experiments at 300 K, show the P and F characters of the first and second group of samples, respectively. The coercive field increases from about 59 Oe up to 108 Oe for $x = 0.50$ and $x = 0.65$, respectively.

Fig. 4 shows the real and imaginary parts of the AC susceptibility versus temperature for all the studied samples. It can be noted in the real part that the $x = 0.25$ and 0.30 samples present broad peaks which are well resolved in two peaks in the imaginary parts. These two peaks are located at 42 and 129 K, 31 and 64 K, 36 and 56 K, for $x = 0.25$, 0.30 and 0.35, respectively. In the case of $x = 0.40$, the curve shows only one peak at 37 K. For the $x = 0.50$ sample the real part of the susceptibility curve shows a plateau which is approximately constant between nearly 40 and 220 K. However, the imaginary part shows a peak at 35 K and a large increase at nearly 220 K. The real part of the $x = 0.55$ sample continuously increases when the temperature increases, with changes of curvature nearly at 30 and 230 K. The imaginary part of the susceptibility confirms a peak at 26 K. Finally, the real part of the susceptibility for the $x = 0.60$ sample presents also a continuous increase with a change of curvature at 22 K which is confirmed by the peak at this temperature showed by its imaginary curve. The low-temperature peaks of the curves can be attributed to a SG transition, as shown in Fig. 5. Here, it is seen that the dependence of the peak position with the frequency for the $x = 0.35$ sample and this peak presents a little shift to higher temperatures when the frequency increases. The high-temperature peaks detected at 129 and 64 K for the $x = 0.25$ and 0.30 samples can be attributed to an AF to P transition in agreement with their high Mn contents and previous results for samples near this composition [12,13]. In this way the SG transition for these samples are of the RSG-AF type and those of the $x = 0.35$ and 0.40 samples are of pure SG type. According to the imaginary part of the AC susceptibility curve for the $x = 0.35$ samples and the previous discussion, one can conclude that for this sample the AF and SG transition temperatures are nearly coincident at 40 K. The high-temperature transitions detected near 220 and 230 K obtained for the $x = 0.50$ and 0.55 samples, respectively, are associated to the blocking temperature of a SP behavior. As shown by Mössbauer results, these samples and that of $x = 0.60$ are ferromagnetic at RT and this explains why their susceptibility curves always increase when the temperature increases. In this way, the SG transition detected at low temperatures for these three samples are of the RSG-F type.

The different magnetic phases in the FeMnAl alloys are due to both their atomic disordered character of the samples, originating from the heat treatment applied during their preparation, and to the competitive and diluted interactions induced

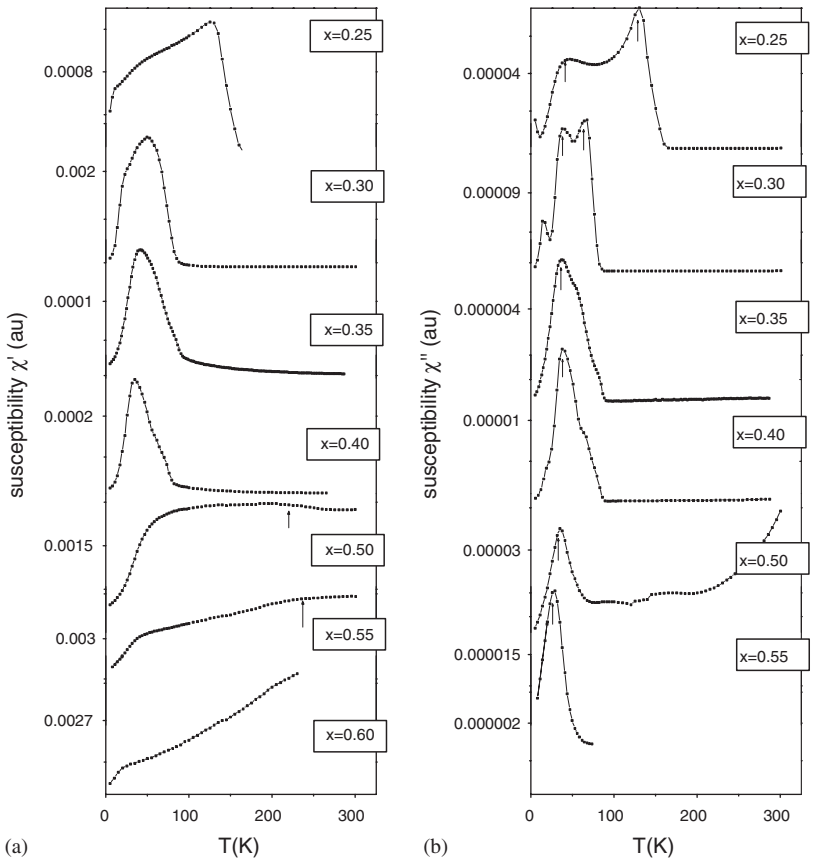

Fig. 4. AC susceptibility curves (a) real part and (b) imaginary part of the $Fe_xMn_{0.65-x}Al_{0.35}$ samples.

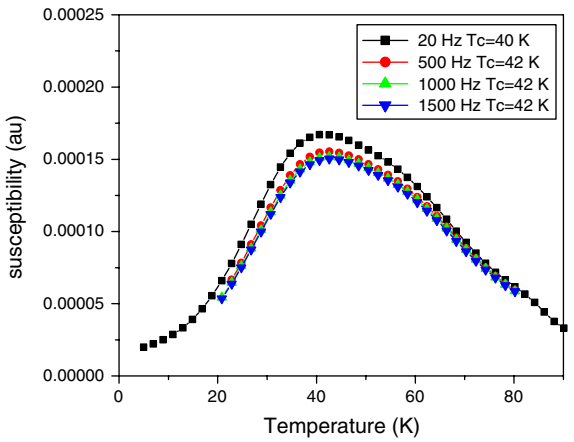

Fig. 5. AC susceptibility curves for the $x = 0.35$ sample at different frequencies.

by the presence of Fe, Mn, and Al atoms. Thus, large Fe contents stabilize the F phase while low Fe contents (high Mn) stabilize the AF phase. However, intermediate Fe contents produce competitive interactions stabilizing the SG phase. Finally, large Fe contents combined to the disordered character yield Fe-rich SP clusters separated by Al-rich grain boundaries.

The different results allow a magnetic phase diagram to be established in the case of FeMnAl alloys. From Fig. 6, one clearly observes an obvious P phase at high temperature, AF at intermediate temperatures (dots) and RSG for low temperatures for low Fe contents (squares). For intermediate Fe contents, only SG behavior is found at low temperatures, while for high Fe

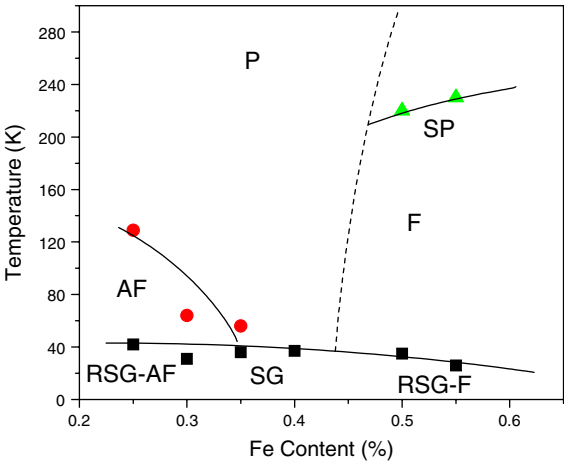

Fig. 6. Proposed magnetic phase diagram for $Fe_xMn_{0.65-x}Al_{0.35}$ disordered system. Full lines are obtained from the theoretical model and the symbols are the experimental results. Dashed lines are suggested according to previous experimental results obtained for alloys with 40 at% Al [24].

contents the phases are P at high temperature, F above about 220 K, SP (triangles) at intermediate temperature (below about 220 K) and RSG at low temperature (squares). It is finally important to emphasize that the limit between the F and SP regions with the P phase (dashed line) is proposed not on the basis of experimental but by analogy to that experimentally obtained for the 40 at% Al series [13].

4. Theoretical model

For this system the proposed model is a diluted and random-site Ising model recalling that the alloys are disordered and that the Al behaves as a magnetic hole, and the Fe and Mn as ferromagnetic and antiferromagnetic, respectively. Then, the proposed Hamiltonian for this ternary magnetic system is based on an Ising model, defined by

$$H = \sum_{\langle i,j \rangle} k_{ij}\sigma_i\sigma_j, \tag{1}$$

where k_{ij} is the reduced exchange interaction $k_{ij} = J_{ij}/k_B T$ with J_{ij} being the corresponding exchange interaction between spins at site i and j, $\sigma_i = \pm 1$, and $\langle i,j \rangle$ states that the sum runs over nearest neighbors. For this ternary disordered system the corresponding site probability distribution is given by

$$P(a_i, \varepsilon_i) = p\delta(a_i)\delta(\varepsilon_i - 1) + x\delta(a_i - 1)\delta(\varepsilon_i) + q\delta(a_i)\delta(\varepsilon_i), \tag{2}$$

where $\delta(a_i)$ is the Dirac delta function and the probability of finding an atom of type a, b or c in the lattice site i is p, x and q, respectively, with

$$p + x + q = 1, \tag{3}$$

and $a_i = 1$, 0 depending whether site i is occupied or not, respectively, by an atom type a and $\varepsilon_i = 1$, 0 depending whether site i is occupied or not, respectively, by an atom type b.

The exchange interaction value k_{ij} depends on the type of atoms located at sites i and j, the atom of the site c is taken as a dilute magnetic site, thus $k_{ac} = k_{ca} = k_{bc} = k_{cb} = k_{cc} = 0$. So for all possible configurations the exchange interaction can be written

$$k_{ij} = (1 - a_i)\varepsilon_i(1 - a_j)\varepsilon_j k_{aa} + (1 - a_i)\varepsilon_i a_j(1 - \varepsilon_j)k_{ab} + a_i(1 - \varepsilon_i)(1 - a_j)\varepsilon_j k_{ba} + a_i(1 - \varepsilon_i)a_j(1 - \varepsilon_j)k_{bb}. \tag{4}$$

The interactions between different atoms are independent of their positions, allowing to assume $k_{ab} = k_{ba}$. For calculating the critical properties of the system we use the MFRG method [18] considering the simplest choice for clusters, namely, one- and two-spin clusters.

5. Theoretical results and discussion

Taking into account the previous experimental results it is possible to obtain theoretically the transitions lines between F–P or AF–P and SG–P by the MFRG method and fitting the exchange interactions.

For the one-spin cluster the Hamiltonian is given by

$$H_1 = -\sum_{i=1}^{z} K_{1i}\sigma_1 b_i \tag{5}$$

for-two-spin cluster it is

$$H_2 = -K_{12}\sigma_1\sigma_2 - \sum_{i=1}^{z-1} K_{1i}\sigma_1 b_{1i} - \sum_{j=2}^{z-1} K_{2j}\sigma_2 b_{2j}, \tag{6}$$

where z is the coordination number of the lattice and b_i and b_{mi} $(m = 1, 2)$ are the effective fields acting on the boundary of the respective cluster. Following the MFRG method it is possible to obtain the magnetization and the Edwards–Anderson SG order parameter for each block. The obtained results after equaling the order parameters for one and two-spin blocks, respectively (the recurrence equations for MFRG [18]), are resumed in the following equation:

$$\varsigma = \begin{cases} 1 & \text{Ferro,} \\ 2 & \text{SpGl,} \end{cases}$$

$$[z-1](p \quad x)\begin{pmatrix} 1 + p\tanh^{\varsigma}(K_{aa}) & x\tanh^{\varsigma}(K_{ab}) \\ p\tanh^{\varsigma}(K_{ba}) & 1 + x\tanh^{\varsigma}(K_{bb}) \end{pmatrix} \begin{pmatrix} K^{\varsigma}_{aa} & K^{\varsigma}_{ab} \\ K^{\varsigma}_{ba} & K^{\varsigma}_{bb} \end{pmatrix} \begin{pmatrix} p \\ x \end{pmatrix} = z(p \quad x)\begin{pmatrix} K^{\varsigma}_{aa} & K^{\varsigma}_{ab} \\ K^{\varsigma}_{ba} & K^{\varsigma}_{bb} \end{pmatrix} \begin{pmatrix} p \\ x \end{pmatrix} \tag{7}$$

with $\xi = 1, 2$ for the F(AF) to P transition, and SG to P transition, respectively. It can be seen that if we take $k_{ij} < 0$ the SG to antiferromagnetic transition is obtained.

Eq. (5) recovers the results already obtained in previous MFRG studies (with the same cluster sizes) reported in Refs. [18,19]. Using this equation with $\xi = 1$ and $k_{ij} < 0$, in order to obtain the AF–P transition curve, the best fit with the experimental data was obtained using the exchange interactions given by $J_{FeFe} = 2.433\,\text{meV}$, $J_{FeMn} = -2.588\,\text{meV}$ and $J_{MnMn} = -2.800\,\text{meV}$. Otherwise, using $\xi = 2$ in order to obtain the SG–P transition curve the best fit was obtained using the exchange interactions $J_{FeFe} = 0.8999\,\text{meV}$, $J_{FeMn} = -1.6502\,\text{meV}$ and $J_{MnMn} = -1.9339\,\text{meV}$. From these results it can be noted that the Fe moments are ferromagnetically coupled, while the Mn moments present an antiferromagnetic interaction between them and with the Fe atoms. Also it is possible to check that the AF interactions are more intensive in the Mn-rich regions with more atoms and less intensive in the Fe-rich regions. Indeed, in this region dominant F interactions compared to AF interactions favor the competition, stabilizing thus the SG phase. If we compare the present exchange interactions obtained values with those reported for $Fe_xMn_{0.7-x}Al_{0.3}$ alloys and with $Fe_{1-x}Al_x$ alloys $(x \leqslant 0.3)$ [10,26], it can be concluded that the present ones are lower and this is a consequence of the higher Al content (35 at%) which dilates the lattice, and consequently decreases the interactions in this way.

Fig. 6 shows the comparison of the experimental (symbols) and the calculated theoretical phase diagram (continuous lines). Good agreement was obtained for the AF–P, AF–SG and P–SG lines. More experiments are now in progress in order to prove the proposed dashed lines for the transitions in the Fe iron-rich side of the magnetic phase diagram, including transitions between F, P, SG and SP phases.

Acknowledgments

The authors are grateful to the Universidad del Valle and Colciencias, Colombian Agency, for partial financial support. C.G. would like to thank the support of Laboratoire de Physique de l'Etat Condensé, Université du Maine, for a research stay. G.A.P.A. would like to thank the support of Centro Brasileiro de Pesquisas Físicas and to CLAF, Centro Latinoamericano de Física, for the research stay and grant, respectively. The present study work was supported by the ECOS-Nord Colombian French exchange program under contract CF99P04.

References

[1] G.L. Kayak, Met. Sci. Heat Treatment 2 (1969) 95.
[2] S.K. Banerji, Met. Prog. April (1978) 59.
[3] P.D. Bilmes, A.C. González, C.L. Llorente, M. Cuyás y Solari, Rev. Metal. Madrid 30 (1994) 298.
[4] G.A. Pérez Alcázar, J.A. Plascak, E. Galvão da Silva, Phys. Rev. B 38 (1988) 2816.
[5] D.J. Chakrabarti, Met. Trans. 8B (1977) 121.
[6] T.V.S.M. Mohan Babu, C. Bansal, Phys. Stat. Sol. (b) 193 (1996) 167.

[7] A. Rosales Rivera, G.A. Pérez Alcázar, J.A. Plascak, Phys. Rev. B 41 (1990) 4774.
[8] M.A. Kobeissi, J. Phys.: Condens. Matter 3 (1991) 4983.
[9] L.E. Zamora, G.A. Pérez Alcázar, A. Bohórquez, J.A. Tabares, J. Magn. Magn. Mater. 137 (1994) 339.
[10] L.E. Zamora, G.A. Pérez Alcázar, A. Bohórquez, J.F. Marco, J.M. González, J. Appl. Phys. 82 (1997) 6165.
[11] H. Bremers, Ch. Jarms, J. Hesse, S. Chajwasiliou, K.G. Efthiadis, Y. Tsonkalas, J. Magn. Magn. Mater. 140 (1995) 63.
[12] L.E. Zamora, G.A. Pérez Alcázar, J.A. Tabares, A. Bohórquez, J.F. Marco, J.M. González, J. Phys. Condens. Matter. 12 (2000) 611.
[13] C. González, G.A. Pérez Alcázar, L.E. Zamora, J.A. Tabares, J.M. Greneche, J. Phys.: Condens. Matter 14 (2002) 6531.
[14] R. Stinchombe, in: C. Domb, M.S. Green (Eds.), Phase Transition and Critical Phenomena, vol. 8, Academic press, London, 1982.
[15] D.P. Belander, Braz. J. Phys. 30 (2000) 682.
[16] W.P. Wolf, Braz. J. Phys. 30 (2000) 794.
[17] A. Pelissetto, E. Vicari, Phys. Rep. 368 (2002) 549.
[18] M. Droz, A. Maritan, A.L. Stella, Phys. Lett. 92A (1982) 287.
[19] M. Lyra, S. Coutinho, Physica A 155 (1989) 232.
[20] J.A. Plascak, W. Figueiredo, B.C.S. Grandi, Braz. J. Phys. 29 (1999) 519.
[21] L.E. Zamora, G.A. Pérez Alcázar, A. Bohórquez, A. Rosales Rivera, J.A. Plascak, Phys. Rev. B. 51 (1995) 9329.
[22] J.A. Plascak, L.E. Zamora, G.A. Pérez Alcázar, Phys. Rev. 61 (2000) 3188.
[23] A. Rosales Rivera, G.A. Pérez Alcázar, J.A. Plascak, Phys. Rev. B 41 (1990) 4774.
[24] C. González, J.M. Greneche, G.A. Pérez Alcázar, A. Hernando Jr., J.M. González, Hyp. Int. 141/142 (2002) 415.
[25] F. Varret, J. Teillet, Unpublished MOSFIT Program.
[26] G.A. Pérez Alcázar, J.A. Plascak, E. Galvão da Silva, Phys. Rev. B 34 (1986) 1940.